RESEARCH ARTICLE

Macromolecular Rapid Communications
www.mrc-journal.de

Photonic Particles Made by the Confined Self-Assembly of a Supramolecular Comb-Like Block Copolymer

Guillaume Moriceau, Cédric Kilchoer, Kenza Djeghdi, Christoph Weder, Ullrich Steiner, Bodo D. Wilts, and Ilja Gunkel**

Approaches that enable the preparation of robust polymeric photonic particles are of interest for the development of nonfading and highly reflective pigments for applications such as paints and display technologies. Here, the preparation of photonic particles that display structural color in both, aqueous suspension and the dry solid state is reported. This is achieved by exploiting the confined self-assembly of a supramolecular comb-like block copolymer (BCP) that microphase separates into a well-ordered lamellar morphology with dimensions that promote a photonic bandgap in the visible range. The comb-like BCP is formed by robust ionic interactions between poly(styrene-*b*-4-vinyl-pyridine) (PS-*b*-P4VP) BCP and dodecylbenzene sulfonic acid (DBSA), which selectively interacts with P4VP blocks. The components are combined in chloroform, and an aqueous emulsion is prepared. Evaporation of the organic solvent leads to the formation of solid microparticles with an onion-like 3D morphology. These photonic pigments display brilliant colors with reflectance spectra featuring pronounced optical bandgaps across the entire visible wavelength range with a peak reflectivity of 80–90%.

1. Introduction

Due to their captivating appearances, nature's vivid structural colors are a long-standing subject of scientific interest.[1,2] Recently, the development of bio-inspired photonic pigments has attracted considerable attention since such materials may be suitable to replace conventional pigments in a broad range of industrial applications. Structural coloration arises from the interaction of light with periodic dielectric materials that are structured on a length scale that is comparable to the wavelength of light, i.e., a few hundred nanometers.[3,4] The optical response of photonic materials can be tailored by their local morphology, dielectric periodicity, and the refractive index contrast between the constituent materials. Structurally colored materials offer high color purity and lightfastness, and can a priori be assembled in a sustainable fashion from environmentally friendly, nontoxic materials. Photonic pigments are therefore of interest for many technological applications, including paints and coatings, optical sensing, display technologies, lasing, and anticounterfeiting.[5–11]

Solution-based, bottom-up self-assembly approaches based on either colloids or block copolymers (BCPs) have recently gained attention for the manufacture of photonic materials.[12–14] BCP self-assembly, in particular, provides convenient access to various nanostructured morphologies, such as lamellae, hexagonally packed cylinders, and gyroids.[15–17] Variation of the molar mass of BCPs allows generating self-assembled morphologies that exhibit a photonic response in the visible range. Confining the self-assembly of such tailored BCPs to a specific geometry allows producing photonic films with tunable coloration and stimuli-responsive properties.[18–26] More recently, the approach has also been used to create photonic fibers and particles.[27–30]

Photonic structures made entirely from linear BCPs suffer from their intrinsically low refractive indices (typically around 1.5) and their high melt viscosity due to the high molar mass that is required for structural periodicities with dimensions in the range of wavelengths of visible light. The low chain mobility of such ultrahigh molar mass BCPs ($M_n > 400$ kg mol^{-1}) usually requires time-consuming postprocessing steps. The low refractive index (contrast) in polymeric photonic structures can, however, be increased by the addition of inorganic high-refractive index materials,[24,31,32] while the low chain mobility can be enhanced by swelling the polymer with additives, such as solvents,[22,26,33] H-bonding and ionic surfactants,[34–36] or by adding low-molar mass homopolymers,[18,37] all of which also increases the periodicity of the photonic structure.

Alternatively, approaches to prepare nanostructures with large and relatively well-ordered domains without the need of annealing or other postprocessing[38] include architectures based on bottle-brush BCPs,[39–41] dendritic BCPs,[42] and supramolecular comb-like BCPs.[21,43] These have denser and significantly more stretched backbones than linear BCPs, which facilitates the generation of morphologies with periodicities in the photonic range. Compared to conventional BCP self-assembly, supramolecular

G. Moriceau, C. Kilchoer, K. Djeghdi, C. Weder, U. Steiner, B. D. Wilts, I. Gunkel
Adolphe Merkle Institute
University of Fribourg
Fribourg 1700, Switzerland
E-mail: bodo.wilts@unifr.ch; ilja.gunkel@unifr.ch

DOI: 10.1002/marc.202100522

assemblies of small molecules and BCPs that interact via H-bonding or ionic interactions employ lower-molar mass BCPs, the higher chain mobility of which increases the self-assembly kinetics and results in good order even after short processing times.

Recently, particles with tunable shapes and internal morphologies were produced by confining BCP self-assembly within emulsion droplets.[44–49] Using this strategy, particles with an internal morphology of concentric lamellae (onion-like microspheres) can be prepared. Due to their spherical shape, such particles hold promise as noniridescent photonic pigments.[30,50–53] Zhu et al. recently prepared such photonic microspheres by emulsifying chloroform solutions of poly(styrene-*b*-2-vinyl-pyridine) (PS-*b*-P2VP), 3-*n*-pentadecylphenol (PDP), and polystyrene in water using a microfluidic device with subsequent solvent evaporation.[52] The PDP hydrogen bonds with the nitrogen atoms of the P2VP blocks, thereby forming supramolecular comb-like macromolecules, which upon solidification microphase separate into onion-like microspheres with alternating concentric domains of P2VP(PDP) and PS. The color of the resulting photonic particles in aqueous suspensions could be tuned across the entire visible spectral range by varying the molar mass of the BCP and the amounts of the additives, while the possibility to retain the structural colors after drying the suspensions remains to be demonstrated. To achieve this, the integrity of the particles, i.e., their composition, shape, and internal structure, must be retained upon drying. In this regard, ionic BCP assemblies, such as supramolecular comb-like complexes of poly(styrene-*b*-4-vinyl-pyridine) (PS-*b*-P4VP) and dodecylbenzene sulfonic acid (DBSA), are of particular interest, as they can form robust solid lamellae with a periodicity that gives rise to a visible bandgap, as previously demonstrated for films.[38]

Here, we report that the confined self-assembly of such supramolecular PS-*b*-P4VP(DBSA) BCPs within μm-sized spheres generates 3D photonic pigments that show structural color in both, suspension and the (dried) solid state. The use of DBSA, which forms strong ionic interactions with the P4VP blocks, yields supramolecular comb-like BCP assemblies that adopt a well-ordered concentric lamellar morphology with a large, constant periodicity, producing structural color. While both suspended and solid particles were predominantly green, some white coloration was observed for the solid particles, likely due to the formation of voids upon drying.

2. Results and Discussion

2.1. Preparation of Photonic Particles Using Supramolecular Comb-Like BCPs

The supramolecular BCP used in this study is made of PS-*b*-P4VP (number-average molar masses, $M_{n,PS}$ = 350 kg mol^{-1} and $M_{n,P4VP}$ = 77 kg mol^{-1}) and dodecylbenzene sulfonic acid (DBSA), which selectively complexes the P4VP blocks via ionic bonding. Complexation with 1 equivalent of DBSA per 4VP unit is expected to afford a symmetric comb-like BCP (weight fractions of ω_{PS} = 0.52 and $\omega_{P4VP(DBSA)}$ = 0.48) with a high total molar mass (M_n = 666 kg mol^{-1}), which is anticipated to self-assemble into a lamellar structure with a periodicity beyond 100 nm (**Figure 1**).

P4VP was favored over P2VP because of its higher glass transition temperature (148 vs 102 °C) and on account of the better accessibility of the nitrogen atoms in the *para* position, which facilitates the protonation and formation of mesomorphic structures.[34,54] DBSA is a commercial, high-boiling point surfactant that is capable of protonating the 4VP monomers, which forms pyridinium ions that strongly interact with sulfonate anions forming a polyelectrolyte.[34,54] The strong ionic interaction between DBSA and P4VP was previously shown to enable the formation of supramolecular comb-like, hierarchical assemblies with comparably large periods, suitable for photonic materials.[21,38] This contrasts with supramolecular assemblies formed by comparatively weak and dynamic H-bonds (e.g., P2VP-PDP), which undergo order–disorder transitions at low temperatures rendering them more suitable for stimuli-responsive systems, such as sensors.[55] To form photonic particles, the self-assembly of lamellae-forming supramolecular comb-like BCPs was confined inside emulsion droplets using a solvent-evaporation-based emulsion technique (Figure 1).[46] Microdroplets were generated using vortex-assisted emulsification of a chloroform solution of comb-like PS-*b*-P4VP(DBSA)$_1$ (30 mg mL^{-1}, 2 wt%) in a continuous aqueous phase containing CTAB (1 mg mL^{-1}) as a surfactant (see the Experimental Section for details and the Supporting Information for a discussion on the optimization of the process). Upon evaporation of chloroform, the droplets shrink and the PS-*b*-P4VP(DBSA)$_1$ concentrates until a critical polymer concentration is reached, upon which the supramolecular BCP self-assembles inside the droplet. After complete evaporation of chloroform (after about 5 days), and the subsequent removal of excess surfactant by centrifugation cycles, polydisperse μm-sized solid particles displaying a vivid coloration were obtained in aqueous suspension (Figure S1A, Supporting Information). The particle diameter varied between 5 and 20 μm. Dry, solid particles were isolated by drop-casting the aqueous suspension of particles onto a glass slide and drying in a vacuum oven at 50 °C (Figure S1B, Supporting Information). The particle composition was determined by ^{1}H NMR and IR spectroscopy (Figures S2 and S3, Supporting Information). The optical properties of the particles were assessed using microspectrophotometry, and their structure was investigated by focused-ion beam scanning electron microscopy (FIB-SEM).

2.2. Optical Properties

Particles show an intense coloration only around their center, which is typical for concentric multilayered systems that are imaged using a microscope with a fixed numerical aperture.[30,50,56] While a variety of bright colors was observed, particles with a green coloration were dominant (Figure S1, Supporting Information). To assess their spectral properties, we measured their local reflectance spectra with a microspectrophotometer. **Figure 2** shows optical micrographs and reflectance spectra of representative particles in suspension (Figure 2A) and in the dried state (Figure 2B). The reflectance spectrum of a typical green particle in suspension displays a sharp reflectance peak around 550 nm with high intensity (up to 90% relative to a silver mirror). In the nonsuspended state, the coloration was preserved and the hue remained unchanged (Figure 2B). The individual

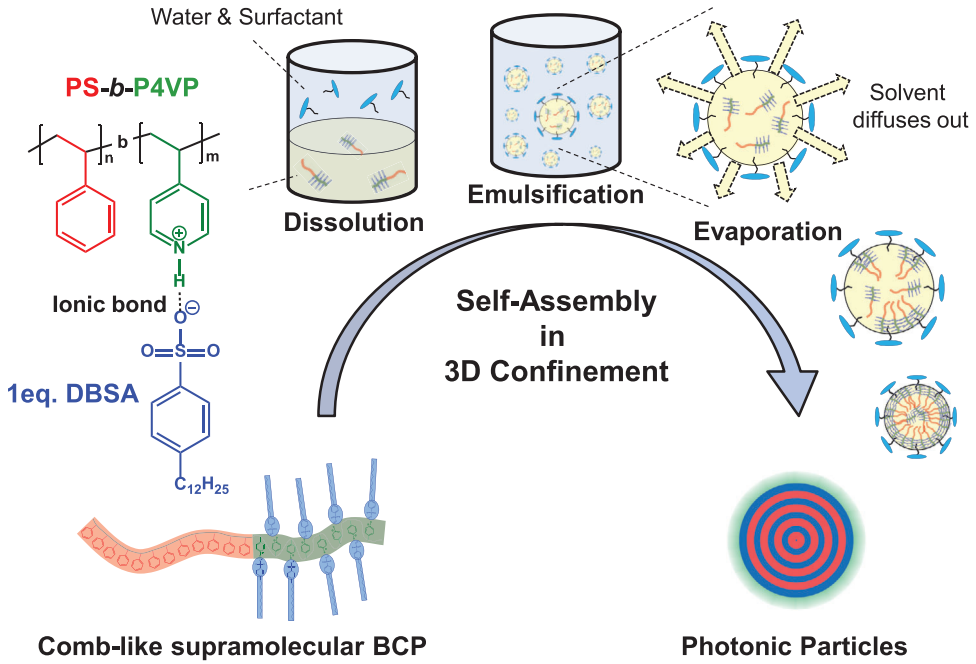

Figure 1. Schematic illustration of the assembly of photonic particles from PS-*b*-P4VP(DBSA)$_1$ comb-like block copolymers (BCPs) using a solvent-evaporation emulsion technique. The supramolecular comb-like BCP is initially dissolved in chloroform (yellow, bottom phase) and mixed with an aqueous solution of the surfactant cetyltrimethylammonium bromide (CTAB; blue, top phase). Surfactant-stabilized droplets are produced by vortex-assisted emulsification. During evaporation, chloroform diffuses out of the droplets and evaporates. The droplets shrink and the BCPs self-assemble. The particles become solid when the solvent evaporation is complete, yielding microparticles with internal nanostructure.

reflection spectra were, however, broadened and lower in intensity compared to the spectra of particles in suspension. We attribute this to the increased refractive index contrast between the particle and its surrounding, as well as changes in particle size and increased variation in the periodicity of the lamellae upon drying. The retention of the green coloration in the dry, nonsuspended state indicates that the periodicity of the internal structure was mostly unchanged when the suspension was dried. Note that maintaining coloration in a dry, nonsuspended state is not necessarily straightforward for polymeric particles due to shrinkage and deformation of the structure that is expected upon evaporation of residual solvent or additives—even water-insoluble PS colloids are known to shrink upon drying.[57] Interestingly, a significant fraction of dry particles appeared white. The reflection spectrum of such a white particle is mostly featureless across the visible spectral range and shows a minor reflectance peak around 500 nm (Figure 2B, gray line).

2.3. Structure of the Particles

To further investigate the structural origin of the green coloration and the scattering of the white particles, the internal morphology of the dried, nonsuspended green and white particles was characterized using FIB-SEM. Prior to FIB-SEM analysis, dried particles were transferred onto carbon tape and the reflection spectra were measured for a green and a white particle (Figure 2B, P1 and P2, respectively). Figure 2C shows the cross-sections of the same green and white particles that were spectrally analyzed. Both particles exhibit a concentric lamellar morphology of alternating layers, which is consistent with the symmetric composition (ω_{PS} = 0.52) of PS-*b*-P4VP(DBSA)$_1$ supramolecular BCPs. The green particle is compact and well-ordered throughout, with an apparent repeat period of 166 ± 33 nm. The white particle shows a similar, layered internal morphology that is, however, partially disrupted by larger porous defects or voids. These microvoids will scatter incident light, and therefore cause the white diffuse appearance of these particles. This is corroborated by the observation that the white appearance of dry particles can be reverted to a green coloration by resuspending the particles in deionized water (Figure S4, Supporting Information). The microvoids seem to open along the interface of individual layers, i.e., perpendicular to the direction of the tension associated with particle shrinkage during vacuum drying. Note that it is possible that microvoids already form during solvent evaporation as the absence of scattering for water-suspended particles might be due to the lower RI contrast compared to nonsuspended particles.[58] The presence of fibrils in these cracks is characteristic of crazing, which is commonly observed for glassy polymers under excessive tensile stresses.[59,60] The observation of "microcrazing" suggests that the cracks arise from drying-induced deformations of the particles in their glassy state. This implies that adjusting the drying rate of suspended particles, or postannealing of dried, nonsuspended particles, might induce healing of the cracks and thereby restore the coloration observed in suspended particles, which certainly warrants further investigations. Notwithstanding, in colloidal particles the complete suppression of particle shrinkage seems difficult and thus distortion and cracking are observed during the assembly of well-ordered colloidal monolayers and dry colloidal crystals.[61]

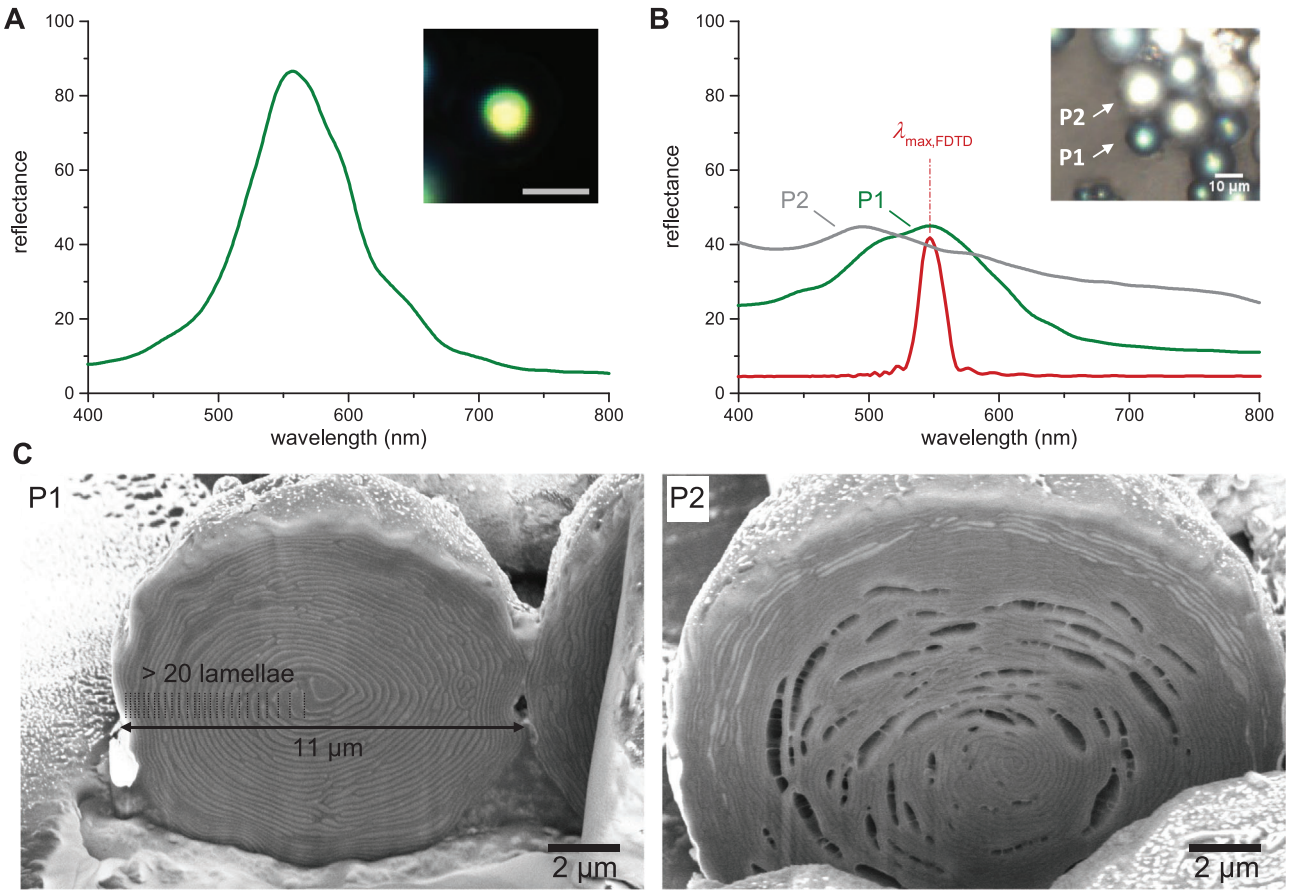

Figure 2. Spectroscopic and structural characterization of self-assembled PS-*b*-P4VP(DBSA)$_1$ microparticles. A) Reflectance spectrum and optical micrograph (inset, scale bar: 10 µm) of a single water-suspended particle of green color, the dominant particle coloration in suspension. B) Reflectance spectra for representative green (P1) and white (P2) particles in the dry, nonsuspended state, along with a simulated spectrum (red curve) using the structural data of P1. C) FIB-SEM images of the cross-sections of the nonsuspended particles P1 and P2 shown in B). While both particles have well-ordered morphologies, the white particle P2 features large internal defects.

2.4. Optical Modeling

To confirm that the particle coloration originates from its concentric lamellar morphology, i.e., structural color, we simulated the reflectance of an idealized 3D concentric multilayer structure using experimentally determined layer thicknesses with an average periodicity of 166 ± 33 nm and tabulated refractive indices n of P4VP (n_{P4VP} = 1.62), DBSA (n_{DBSA} = 1.51), and PS (n_{PS} = 1.59) (Figure 2B, red line).[52] A peak reflectance at 550 nm with a half-width of ≈50 nm is obtained by this simulation. Figure S5 (Supporting Information) shows the angle-dependent reflectance and highlights that a significant broadening of the reflectance only occurs for very large measurement apertures. The simulated values are consistent with the spectral data, although the experimental spectra are broader, which is attributed to local structural variations, including varying layer thicknesses. This implies that the optical properties are effectively dictated by the composition and structural properties of the particles, which are directly related to the molecular structure of the PS-*b*-P4VP(DBSA)$_1$ supramolecular BCPs.

2.5. A Variety of Colors

While most of the particles showed green coloration, a small fraction of both suspended and nonsuspended particles displayed other colors from the entire visible wavelength range (Figure S1, Supporting Information). Their reflectance spectra (**Figure 3**) show peaks that are bathochromically and hypsochromically shifted with respect to the predominantly green particles shown in Figure 2. The spectra of particles in suspension show sharp, high-intensity peaks, while broader peaks and lower reflectance are observed for nonsuspended particles. Given all samples were prepared using the same PS-*b*-P4VP, the change in lamellar spacing leading to differently colored particles likely arises from occasional local deviations in the stoichiometrically defined DBSA content but can also be due to the presence of surfactant or residual solvent inside these particles. The observation of color over the full visible range implies that color tunability is feasible in this system, which warrants further investigation.

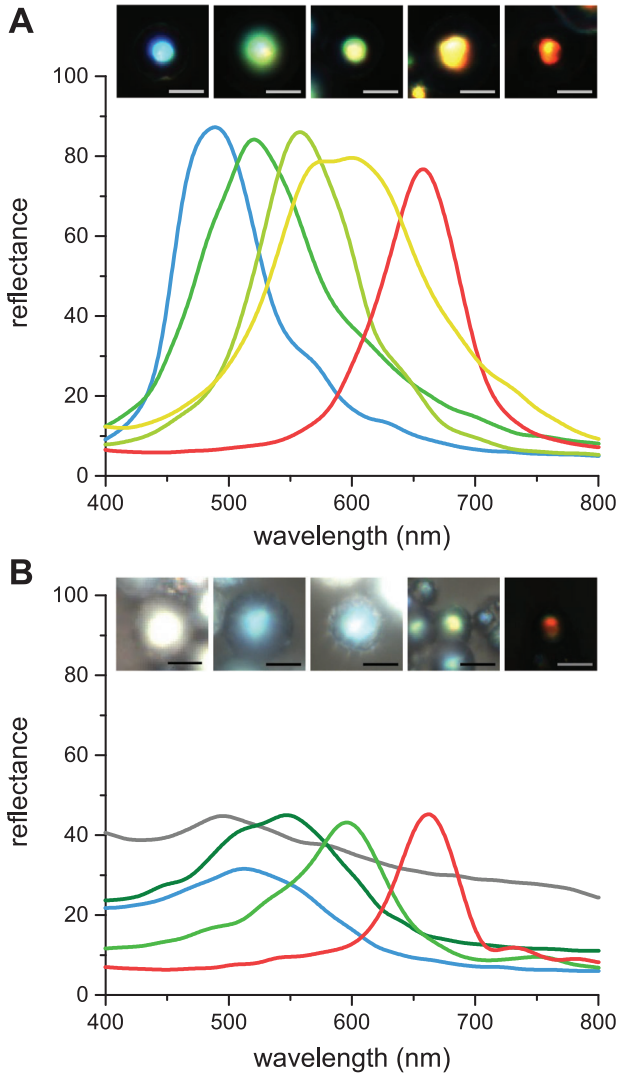

Figure 3. Optical micrographs (scale bars: 10 µm) and corresponding reflectance spectra (shown in the color observed in the micrographs) of individual particles of various coloration A) in suspension and B) in the dry, nonsuspended solid state.

3. Conclusion

In conclusion, we demonstrate a facile preparation process that affords photonic particles based on a supramolecular comb-like BCP of PS-*b*-P4VP functionalized with DBSA. The strong ionic interaction between DBSA and the 4VP monomers enables the formation of a robust, comb-like supramolecular BCP that self-assembles into concentric lamellar morphologies (onion-like layered internal microstructure) in the confinement of μm-sized particles. The preparation of such particles was achieved by confining the self-assembly of supramolecular comb-like PS-*b*-P4VP(DBSA) BCPs into an emulsion droplet exploiting a facile solvent-evaporation emulsion technique in the presence of a suitable surfactant. The resulting particles display structural color in aqueous suspension as well as in the dry, nonsuspended state. While most particles showed a green coloration when suspended in water, a significant fraction of the nonsuspended particles appeared white, which is attributed to voids and cracks that were formed in the particles upon removing them from suspension. Despite these defects, the internal onion-like morphology of the microparticles was preserved. In the absence of cracks, a similar green coloration was observed for both suspended and nonsuspended particles, demonstrating the robust structural color obtained in these supramolecular polymeric assemblies.

Such structurally colored polymeric particles hold promise for applications in displays, paints, and coatings. To this end, the work presented here should be further extended in terms of color tunability and the suppression of crack formation in self-assembled supramolecular BCP microparticles by adjusting the DBSA content and further investigating the drying process, as this would enable the routine synthesis of photonic pigments in the solid state.

4. Experimental Section

Materials: The PS_{350k}-*b*-$P4VP_{77k}$ BCP (M_n = 427 kg mol^{-1} – $Đ$ = 1.15) was purchased from Polymer Source, Inc. (Dorval, Canada) and used without further purification. 4-Dodecylbenzenesulfonic acid (DBSA – mixture of C10-13 isomers – ≥95%), cetyltrimethylammonium bromide (CTAB – ≥98%), sodium dodecylbenzenesulfonate (SDBS – technical grade), poly(vinyl alcohol) (PVA – M_w = 13–23 kg mol^{-1} — 87–89% hydrolyzed), sodium dodecyl sulfate (SDS), and Tween20 were obtained from Sigma-Aldrich and used as received.

Preparation of Supramolecular Comb-Like BCPs: PS_{350k}-*b*-$P4VP_{77k}$ BCP was dissolved in chloroform and stirred overnight to afford homogeneous stock solutions (30 and 40 mg mL^{-1}). A stock solution of DBSA (50 mg mL^{-1}) in chloroform was prepared in parallel. Supramolecular comb-like PS-*b*-P4VP(DBSA)$_1$ BCPs were prepared by mixing the premade stock solutions of PS-*b*-P4VP in chloroform with the DBSA stock solution in chloroform (50 mg mL^{-1}) to afford the desired molar ratio between DBSA and P4VP units (1 equivalent). The total solid concentration was adjusted to a desired value (20–40 mg mL^{-1}) by adding chloroform. The mixture was stirred overnight at room temperature (21°C) to allow equilibration of a supramolecular comb-like structure.

Surfactant solutions (continuous phase) were prepared by dissolution of the surfactants (SDS, CTAB, SDBS, PVA, and Tween20) in deionized (DI) water at predetermined concentration, stirred overnight at room temperature, and filtered before use.

Preparation of Photonic Microspheres by Emulsion-Evaporation Using Vortex Emulsification: The emulsion was prepared by mixing 0.5 mL of the polymer formulation (organic dispersed phase) with 3 mL of surfactant solution (continuous phase) in a 7 mL screw-cap vial, and by vortexing at 3000 rpm during 15 s. The resulting emulsion was transferred into a Petri dish (ø = 5 cm — PD5) and diluted with 15 mL DI water (height ≈0.8 cm) (see the Supporting Information for a discussion on the optimization of the process). The PD5 was then covered and left at room temperature (21 °C) in a ventilated hood for about 5 days to allow slow evaporation of the organic solvent. The suspension was subsequently transferred to a centrifuge tube and the excess of surfactant was removed by repeated washing. Three cycles of centrifugation (at 9000 rpm, for 10 min), supernatant removal and redispersion in DI water (3–5 mL) were performed. The solid particles were stored as a suspension in DI water before characterization. Dry, solid particles were isolated by drop-casting the aqueous suspension of particles onto a glass slide and drying in a vacuum oven at 50 °C.

Optical Characterization: Optical microscopy and microspectroscopy were performed using a customized Zeiss Axio Scope.A1 polarized light microscope and a Point Grey GS3-U3-28S5C-C CCD camera (FLIR Integrated Imaging Solutions Inc., Richmond, CA). A halogen lamp (Zeiss HAL100) or Xenon lamp (SLS401, Thorlabs, Ely, UK) was used as light

source in Koehler illumination for all measurements. The particles in suspension were imaged on glass slides covered with a glass slip or directly in suspension using an 40x water-immersion objective (OlympusUMPlanFL). For dry-state imaging of nonsuspended particles, particles in suspension were deposited on glass slide and dried at 50 °C under vacuum before imaging. Images were recorded in reflection in bright field.

The spectral reflectance was measured on the same equipment, where an optical fiber (Avantes, QP50-2-UV-BX, 50 µm core size) was placed confocal to the image plane. The other end of the fiber was coupled to a diode-array spectrometer (QEPro; Ocean Insight, Dunedin, FL). The reflectance spectra were normalized against a silver mirror (Thorlabs, PF10-03-P01, avg. reflectance >97.5% for $\lambda = 450$–2000 nm). The spectral data were collected in reflection mode (bright field) using a high NA objective (Zeiss, LD EC Epiplan-Neofluar, 50x, NA 0.8).

Structural Characterization: The particles were cut open using a focused-ion beam (FIB) and their internal morphology was imaged with a FEI Scios 2 dual-beam SEM equipped with a Ga^+ ion column and a field-emission electron gun (FEI, Eindhoven, the Netherlands). The samples were first mounted on aluminum stubs using conductive carbon tape and coated with a 5 nm thick layer of Au using a sputter coater (Cressington 208HR, Cressington Scientific Instruments, Watford, England). Several detectors (EDT, T1, or T2) and imaging voltage (2 or 5 kV) were used.

Optical Simulations: 3D optical modeling was performed with a finite-difference time-domain (FDTD) method using commercial software (Finite Difference IDE, Release 2021 R.1.1; Ansys Lumerical Software ULC, Canada). An idealized concentric PS/P4VP multilayer structure using a lamellar period determined from SEM image analysis (ImageJ v. 1.58h., the lamellar period was obtained by averaging 20 consecutive lamellae at 10 different locations) was created. In the 3D FDTD simulation, unpolarized plane-wave illumination (400–800 nm) and a mesh size of 5 nm was considered. Power monitors placed behind the source were used to collect the reflected power. The numerical aperture dependence was calculated from the simulated far-field scattering pattern using a custom-written routine in Matlab (v2020a, Mathworks).

Characterization of Particle Composition: Prior to characterization, the particles suspension in water was freeze-dried. ^{1}H-NMR spectroscopy was recorded in deuterated chloroform ($CDCl_3$) using a Bruker Avance DPX-400 NMR Spectrometer. FTIR spectra were recorded with a Perkin Elmer Spectrum 65 FTIR spectrometer and analyzed with the accompanying Perkin Elmer Spectrum 10 software.

Supporting Information

Supporting Information is available from the Wiley Online Library or from the author.

Acknowledgements

This study was financially supported by the Swiss National Science Foundation (SNSF) through the National Center of Competence (NCCR) in Research Bio-Inspired Materials (Grant No. 51NF40-182881), the ERC Advanced Grant PrISMoID, and the Adolphe Merkle Foundation.

Open access funding provided by Universite de Fribourg.

Conflict of Interest

The authors declare no conflict of interest.

Author Contributions

C.W. and U.S. conceived the project; G.M., C.K., K.D., and B.D.W. performed and analyzed measurements; G.M., B.D.W., and I.G. wrote the first draft of the paper; all authors revised the manuscript and approved the final version.

Data Availability Statement

The data that support the findings of this study are openly available in Zenodo repository at https://doi.org/10.5281/zenodo.5517508, reference number 5517508.

Keywords

3D confined self-assembly, photonic particles, structural colors, supramolecular comb-like block copolymers

Received: August 14, 2021
Revised: September 10, 2021
Published online: September 23, 2021

[1] S. Kinoshita, S. Yoshioka, J. Miyazaki, *Rep. Prog. Phys.* **2008**, *71*, 076401.
[2] M. Srinivasarao, *Chem. Rev.* **1999**, *99*, 1935.
[3] S. Kinoshita, S. Yoshioka, *ChemPhysChem* **2005**, *6*, 1442.
[4] Y. Fu, C. A. Tippets, E. U. Donev, R. Lopez, *Wiley Interdiscip. Rev. Nanomed. Nanobiotechnol.* **2016**, *8*, 758.
[5] Y. Zhao, Z. Xie, H. Gu, C. Zhu, Z. Gu, *Chem. Soc. Rev.* **2012**, *41*, 3297.
[6] A. G. Dumanli, T. Savin, *Chem. Soc. Rev.* **2016**, *45*, 6698.
[7] S. Tadepalli, J. M. Slocik, M. K. Gupta, R. R. Naik, S. Singamaneni, *Chem. Rev.* **2017**, *117*, 12705.
[8] M. Kolle, S. Lee, *Adv. Mater.* **2018**, *30*, 1702669.
[9] W. Hong, Z. Yuan, X. Chen, *Small* **2020**, *16*, 1907626.
[10] H. Song, K. Singer, J. Lott, Y. Wu, J. Zhou, J. Andrews, E. Baer, A. Hiltner, C. Weder, *J. Mater. Chem.* **2009**, *19*, 7520.
[11] K. D. Singer, T. Kazmierczak, J. Lott, H. Song, Y. Wu, J. Andrews, E. Baer, A. Hiltner, C. Weder, *Opt. Express* **2008**, *16*, 10358.
[12] J. F. Galisteo-López, M. Ibisate, R. Sapienza, L. S. Froufe-Pérez, Á. Blanco, C. López, *Adv. Mater.* **2011**, *23*, 30.
[13] M. Stefik, S. Guldin, S. Vignolini, U. Wiesner, U. Steiner, *Chem. Soc. Rev.* **2015**, *44*, 5076.
[14] E. S. A. Goerlitzer, R. N. Klupp Taylor, N. Vogel, *Adv. Mater.* **2018**, *30*, 1706654.
[15] F. S. Bates, M. A. Hillmyer, T. P. Lodge, C. M. Bates, K. T. Delaney, G. H. Fredrickson, *Science* **2012**, *336*, 434.
[16] C. M. Bates, F. S. Bates, *Macromolecules* **2017**, *50*, 3.
[17] C. Cummins, R. Lundy, J. J. Walsh, V. Ponsinet, G. Fleury, M. A. Morris, *Nano Today* **2020**, *35*, 100936.
[18] A. Urbas, R. Sharp, Y. Fink, E. L. Thomas, M. Xenidou, L. J. Fetters, *Adv. Mater.* **2000**, *12*, 812.
[19] A. C. Edrington, A. M. Urbas, P. Derege, C. X. Chen, T. M. Swager, N. Hadjichristidis, M. Xenidou, L. J. Fetters, J. D. Joannopoulos, Y. Fink, E. L. Thomas, *Adv. Mater.* **2001**, *13*, 421.
[20] C. Osuji, C.-Y. Chao, I. Bita, C. K. Ober, E. L. Thomas, *Adv. Funct. Mater.* **2002**, *12*, 753.
[21] S. Valkama, H. Kosonen, J. Ruokolainen, T. Haatainen, M. Torkkeli, R. Serimaa, G. Ten Brinke, O. Ikkala, *Nat. Mater.* **2004**, *3*, 872.
[22] Y. Kang, J. J. Walish, T. Gorishnyy, E. L. Thomas, *Nat. Mater.* **2007**, *6*, 957.
[23] J. Ge, Y. Yin, *Angew. Chem., Int. Ed.* **2011**, *50*, 1492.
[24] S. Guldin, M. Kolle, M. Stefik, R. Langford, D. Eder, U. Wiesner, U. Steiner, *Adv. Mater.* **2011**, *23*, 3664.
[25] A. Noro, Y. Tomita, Y. Matsushita, E. L. Thomas, *Macromolecules* **2016**, *49*, 8971.
[26] Y. Xu, R. J. Hickey, *Macromolecules* **2020**, *53*, 5711.
[27] J.-H. Lee, C. Y. Koh, J. P. Singer, S.-J. Jeon, M. Maldovan, O. Stein, E. L. Thomas, *Adv. Mater.* **2014**, *26*, 532.

[28] A. J. Parnell, J. P. A. Fairclough, in *Organic and Hybrid Photonic Crystals* (Ed: D. Comoretto), Springer International Publishing, Cham **2015**, pp. 127–143.
[29] M. Malekovic, M. Urann, U. Steiner, B. D. Wilts, M. Kolle, *Adv. Opt. Mater.* **2020**, *8*, 2000165.
[30] Y. Yang, H. Kim, J. Xu, M.-S. Hwang, D. Tian, K. Wang, L. Zhang, Y. Liao, H.-G. Park, G.-R. Yi, X. Xie, J. Zhu, *Adv. Mater.* **2018**, *30*, 1707344.
[31] M. Bockstaller, R. Kolb, E. L. Thomas, *Adv. Mater.* **2001**, *13*, 1783.
[32] S. Y. Choi, M. Mamak, G. Von Freymann, N. Chopra, G. A. Ozin, *Nano Lett.* **2006**, *6*, 2456.
[33] A. Noro, Y. Tomita, Y. Shinohara, Y. Sageshima, J. J. Walish, Y. Matsushita, E. L. Thomas, *Macromolecules* **2014**, *47*, 4103.
[34] O. Ikkala, J. Ruokolainen, G. Ten Brinke, M. Torkkeli, R. Serimaa, *Macromolecules* **1995**, *28*, 7088.
[35] J. Ruokolainen, G. Ten Brinke, O. Ikkala, M. Torkkeli, R. Serimaa, *Macromolecules* **1996**, *29*, 3409.
[36] J. Ruokolainen, *Science* **1998**, *280*, 557.
[37] G. S. Doerk, R. Li, M. Fukuto, K. G. Yager, *Macromolecules* **2020**, *53*, 1098.
[38] H. Kosonen, S. Valkama, J. Ruokolainen, M. Torkkeli, R. Serimaa, G. Ten Brinke, O. Ikkala, *Eur. Phys. J. E* **2003**, *10*, 69.
[39] A. L. Liberman-Martin, C. K. Chu, R. H. Grubbs, *Macromol. Rapid Commun.* **2017**, *38*, 1700058.
[40] D.-P. Song, G. Jacucci, F. Dundar, A. Naik, H.-F. Fei, S. Vignolini, J. J. Watkins, *Macromolecules* **2018**, *51*, 2395.
[41] Y.-L. Li, X. Chen, H.-K. Geng, Y. Dong, B. Wang, Z. Ma, L. Pan, G.-Q. Ma, D.-P. Song, Y.-S. Li, *Angew. Chem. Int.* **2021**, *60*, 3647.
[42] B. M. Boyle, T. A. French, R. M. Pearson, B. G. Mccarthy, G. M. Miyake, *ACS Nano* **2017**, *11*, 3052.
[43] O. Ikkala, *Science* **2002**, *295*, 2407.
[44] S.-J. Jeon, G.-R. Yi, S.-M. Yang, *Adv. Mater.* **2008**, *20*, 4103.
[45] R. Deng, S. Liu, J. Li, Y. Liao, J. Tao, J. Zhu, *Adv. Mater.* **2012**, *24*, 1889.
[46] K. H. Ku, J. M. Shin, H. Yun, G.-R. Yi, S. G. Jang, B. J. Kim, *Adv. Funct. Mater.* **2018**, *28*, 1802961.
[47] N. Yan, Y. Zhu, W. Jiang, *Chem. Commun.* **2018**, *54*, 13183.
[48] C. K. Wong, X. Qiang, A. H. E. Müller, A. H. Gröschel, *Prog. Polym. Sci.* **2020**, *102*, 101211.
[49] J. J. Shin, E. J. Kim, K. H. Ku, Y. J. Lee, C. J. Hawker, B. J. Kim, *ACS Macro Lett.* **2020**, *9*, 306.
[50] D.-P. Song, T. H. Zhao, G. Guidetti, S. Vignolini, R. M. Parker, *ACS Nano* **2019**, *13*, 1764.
[51] Q. He, K. H. Ku, H. Vijayamohanan, B. J. Kim, T. M. Swager, *J. Am. Chem. Soc.* **2020**, *142*, 10424.
[52] Y. Yang, T.-H. Kang, K. Wang, M. Ren, S. Chen, B. Xiong, J. Xu, L. Zhang, G.-R. Yi, J. Zhu, *Small* **2020**, *16*, 2001315.
[53] T. H. Zhao, G. Jacucci, X. Chen, D.-P. Song, S. Vignolini, R. M. Parker, *Adv. Mater.* **2020**, *32*, 2002681.
[54] J. Ruokolainen, M. Torkkeli, R. Serimaa, S. Vahvaselkä, M. Saariaho, G. Ten Brinke, O. Ikkala, *Macromolecules* **1996**, *29*, 6621.
[55] J. Ruokolainen, M. Torkkeli, R. Serimaa, E. Komanschek, G. Ten Brinke, O. Ikkala, *Macromolecules* **1997**, *30*, 2002.
[56] N. Vogel, S. Utech, G. T. England, T. Shirman, K. R. Phillips, N. Koay, I. B. Burgess, M. Kolle, D. A. Weitz, J. Aizenberg, *Proc. Natl. Acad. Sci. USA* **2015**, *112*, 10845.
[57] A. L. Volynskii, N. F. Bakeev, *Solvent Crazing of Polymers*, Elsevier, Amsterdam, New York **1995**.
[58] K. H. Ku, J. M. Shin, D. Klinger, S. G. Jang, R. C. Hayward, C. J. Hawker, B. J. Kim, *ACS Nano* **2016**, *10*, 5243.
[59] E. J. Kramer, L. L. Berger, in *Crazing in Polymers*, *Vol. 2*, Springer, Berlin, Heidelberg **1990**, pp. 1–68.
[60] M. M. Ito, A. H. Gibbons, D. Qin, D. Yamamoto, H. Jiang, D. Yamaguchi, K. Tanaka, E. Sivaniah, *Nature* **2019**, *570*, 363.
[61] J. Zhang, Z. Sun, B. Yang, *Curr. Opin. Colloid Interface Sci.* **2009**, *14*, 103.

